Keck II adaptive optics upgrade: simulations of the near-infrared pyramid sensor

Cedric Plantet, Charlotte Z. Bond, Christophe Giordano, Guido Agapito, Mojtaba Taheri, et al.

Cedric Plantet, Charlotte Z. Bond, Christophe Giordano, Guido Agapito, Mojtaba Taheri, Simone Esposito, Peter Wizinowich, "Keck II adaptive optics upgrade: simulations of the near-infrared pyramid sensor," Proc. SPIE 10703, Adaptive Optics Systems VI, 1070335 (17 July 2018); doi: 10.1117/12.2313190

SPIE.

Event: SPIE Astronomical Telescopes + Instrumentation, 2018, Austin, Texas, United States

Keck II adaptive optics upgrade: simulations of the near-infrared pyramid sensor

Cedric Plantet[a], Charlotte Z. Bond[b], Christophe Giordano[a], Guido Agapito[a], Mojtaba Taheri[c], Simone Esposito[a], and Peter Wizinowich[d]

[a]INAF - Osservatorio Astrofisico di Arcetri, 50125 Firenze, Italy
[b]Institute for Astronomy, University of Hawaii, 640 N. Aohoku Place, Hilo, HI 96720
[c]University of Victoria - NRC Herzberg, Victoria, Canada
[d]W. M. Keck Observatory, 65-1120 Mamalahoa Hwy., Kamuela, HI 96743, USA

ABSTRACT

A future upgrade of the Keck II telescope's adaptive optics system will include a near-infrared pyramid wavefront sensor. It will benefit from low-noise infrared detector technology, specifically the avalanche photodiode array SAPHIRA (Leonardo). The system will either operate with a natural guide star in a single conjugated adaptive optics system, or using a laser guide star (LGS), with the pyramid working as a low-order sensor. We present a study of the pyramid sensor's performance via end-to-end simulations, including an analysis of calibration strategies. For LGS operation, we compare the pyramid to LIFT, a focal-plane sensor dedicated to low-order sensing.

Keywords: Adaptive optics, Wavefront sensing, Infrared, Keck, Pyramid, LIFT

1. INTRODUCTION

A future upgrade of the Keck II telescope's Adaptive Optics (AO) system[1] will include a pyramid Wavefront Sensor (WFS)[2] working in the near-infrared (J and H band).[3] The main goal of this upgrade is to perform direct imaging and slit spectroscopy of exoplanets around M dwarfs. The flux from these stars is very faint at optical wavelengths, but sufficient in the near-infrared to use them as Natural Guide Stars (NGS) in a single conjugated AO system, given the adequate detector technology. The overall performance of this new AO system will also benefit from the advantages of sensing in the infrared, compared to the visible: a well corrected Point Spread Function (PSF) on the tip of the pyramid will allow greater sensitivity; and access to redder stars and stars behind dust clouds will provide greater sky coverage. The recently developed avalanche photodiode arrays, such as the SAPHIRA (Leonardo), provide a low noise (< 1 e- at high avalanche gain) and are thus suitable for this application.[4] In addition to this NGS mode, the system will also provide a LGS (Laser Guide Star) mode. In this case, the pyramid would be used as a Low-Order (LO) sensor only.

In a previous paper[5] we have presented end-to-end simulations of the infrared pyramid with PASSATA.[6] In NGS mode, the pyramid should provide a Strehl Ratio (SR) in K band of more than 80% at the bright end and around 25% at the faint end (magnitude H = 14). In LGS mode, the pyramid would not benefit from a hardware rebin of pixels, and a focal plane sensor would be preferable to estimate low orders. A comparison with LIFT[7,8] has demonstrated a gain of 2 magnitudes for tip/tilt sensing up to 15" off axis and a similar performance for focus (in median conditions). This previous study[5] did not take into account chromatic dispersion from the atmosphere or from the pyramid itself.

Here we present an updated version of the previous simulations. The update includes the impact of chromatic dispersion, in order to determine whether an Atmospheric Dispersion Compensator (ADC) is required. We also report on simulations used to inform the design and optical requirements of the Keck pyramid system, specifically the resolution of the pyramid sensor, to reduce sensitivity to mis-registration, and the effect of optical aberrations, such as expected Non-Common Path Aberrations (NCPA). Finally we discuss potential calibration strategies and the initial use of the Keck calibration source to measure response matrices and close the loop on-sky.

Further author information:
C.P.: E-mail: plantet@arcetri.astro.it

Adaptive Optics Systems VI, edited by Laird M. Close, Laura Schreiber, Dirk Schmidt, Proc. of SPIE Vol. 10703, 1070335 · © 2018 SPIE
CCC code: 0277-786X/18/$18 · doi: 10.1117/12.2313190

2. END-TO-END SIMULATIONS

Here we summarize the expected performance of the Keck pyramid WFS. In NGS mode we consider the impact of atmospheric dispersion, whilst the performance in LGS mode is compared with LIFT.

2.1 Simulation parameters

The simulation parameters are the following:

- Sensing band: H (1500-1800 nm).
- Transmission to detector + quantum efficiency: 0.3.
- Magnitude (if not specified): 14.
- Seeing (at 500 nm at zenith): 0.55".
- Pyramid's Field of View (FoV) diameter: 2". The FoV is limited to reduce sky background.
- Pyramid pupil sampling: 40×40.
- Max. number of corrected modes: 250. This is less than what the deformable mirror (with 32×32 actuators) can correct, but we are limited by the pyramid's FoV. The mode basis includes the 5 first Zernike modes, the others are Karhunen-Loève modes.
- RON: 1 e-.
- Dark current: 20 e-/s.
- Sky background (H band): 14 mag/arcsec^2.
- M1 co-phasing error: 60 nm of high-order aberrations (non-measured by the WFS).
- Pyramid dispersion in H: pupil shift of 0.25 pixel.

The tilt due to the atmospheric chromatic dispersion is reported in Table 2, at different wavelengths. We orientate the dispersion either along the X axis or at 45°.

Table 1. C_n^2 profile.

Altitude (km)	0	0.5	1	2	4	8	16
C_n^2 (%)	51.7	11.9	6.3	6.1	10.5	8.1	5.4

Table 2. Tilt due to the atmospheric chromatic dispersion.

	Zenith angle (deg)	Wavelength (nm)				
		1500	1565	1630	1715	1800
Tilt amplitude (nm)	30	103.5	48.5	0	-55.3	102.9
	60	310.6	145.6	0	165.9	308.7

2.2 NGS mode

The expected Strehl ratios in K band for the NGS mode are given in Table 3 for the bright end (an H-band magnitude of 10) and in Table 4 for the faint end (an H-band magnitude of 14). The optimized number of corrected modes, modulation radius and frequency are indicated for each case. The optimization is done by simply exploring the parameters in the simulation and selecting the best result.

Table 3. Strehl ratio in NGS mode at magnitude H=10, with the corresponding optimized parameters.

Zenith angle (deg)	Dispersion	SR in K (%)	Num. modes	Modulation radius (λ/D)	Frequency (Hz)
30	None	84.8	250	1.5	500
	Along X	84.5	250	1.0	500
	At 45°	84.8	250	1.5	500
60	None	79.0	250	1.5	500
	Along X	78.9	250	1.5	500
	At 45°	78.9	250	1.5	500

Table 4. Strehl ratio in NGS mode at magnitude H=14, with the corresponding optimized parameters.

Zenith angle (deg)	Dispersion	SR in K (%)	Num. modes	Modulation radius (λ/D)	Frequency (Hz)
30	None	30.3	77	2.5	200
	Along X	30.8	77	3.0	200
	At 45°	31.3	77	3.0	200
60	None	22.2	104	3.5	200
	Along X	22.2	119	3.5	200
	At 45°	22.2	104	3.5	200

The expected SR ranges between 30% (faint end) and 85% (bright end) at a zenith angle of 30° and between 22% and 79% at a zenith angle of 60°. This is in agreement with previous results.[5] We notice that the pyramid is insensitive to the chromatic dispersion, even at low elevation. We can thus conclude that no ADC is needed to achieve a good performance with the Pyramid WFS.

2.3 LGS mode

In LGS mode, the pyramid will measure only low-order aberrations up to focus. In this section, we compare the performance of the pyramid and LIFT for the estimation of low orders, at a zenith angle of 30° (median case, Fig. 1) or 60° (bad case, Fig. 2), with the optimized parameters (frequency and modulation radius) given in Table 5 and Table 6. LIFT measures tip/tilt and focus from a single PSF with a known astigmatism. The algorithm itself is a maximum-likelihood estimator, linearized with a small phase approximation.[7,8]

We consider two operational cases: only tip/tilt estimated and corrected or a full estimation/correction of tip/tilt and focus. Some additional parameters and assumptions apply in LGS mode:

- Point-source LGS.
- Tip/tilt input: turbulence + LGS jitter of 106 mas rms.
- Focus input (none in "only tip/tilt" cases): residual from LGS sensing + sinusoid of amplitude 100 nm and period 5 seconds (very rough approximation of the sodium altitude variation).
- No truth sensing for modes above focus.

- LIFT's pixel scale: 10 mas. This pixel scale was chosen to match the f-number at the tip of the pyramid, so that both sensors could use the same camera. It approximately corresponds to $\lambda/3D$ per pixel.

In the following figures, the tip/tilt is given in nm rms. The conversion to mas is: 12 nm rms = 1 mas. The diffraction limit in H is $\lambda/D = 34$ mas.

Table 5. Optimized parameters for the LGS mode at z = 30°.

		Pyramid		LIFT
		Modulation radius (λ/D)	Frequency (Hz)	Frequency (Hz)
0"	No disp.	0	333	333
	Disp. X	0	333	333
	Disp. 45°	0	333	333
15"	No disp.	0	500	333
	Disp. X	0	500	333
	Disp. 45°	0	333	333
40"	No disp.	1	200	333
	Disp. X	1	200	333
	Disp. 45°	1	200	200

Table 6. Optimized parameters for the LGS mode at z = 60°.

		Pyramid		LIFT
		Modulation radius (λ/D)	Frequency (Hz)	Frequency (Hz)
0"	No disp.	0	500	200
	Disp. X	1	200	200
	Disp. 45°	1	200	200
15"	No disp.	1	333	200
	Disp. X	1	200	200
	Disp. 45°	1	333	200
40"	No disp.	1	200	200
	Disp. X	1	333	200
	Disp. 45°	1	200	200

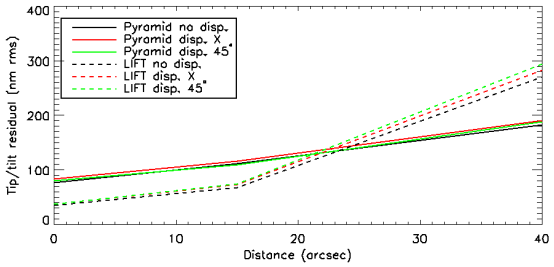

(a) Only tip/tilt estimated

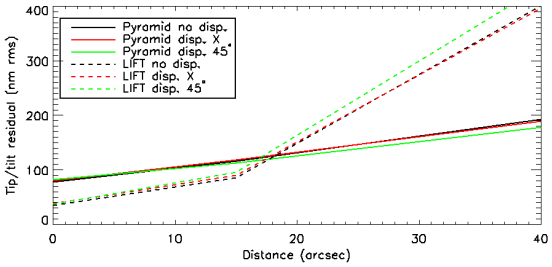

(b) Tip/tilt/focus estimated, tip/tilt res.

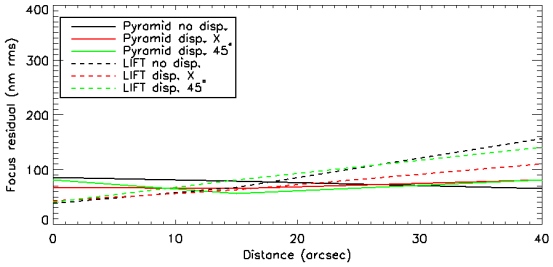

(c) Tip/tilt/focus estimated, focus res.

Figure 1. Comparison of the LO residuals obtained with LIFT or the pyramid for different dispersion conditions: no dispersion, dispersion along X or dispersion at 45°. Top left: Only tip/tilt estimated. Top right and bottom: tip/tilt and focus residuals when the 3 modes are estimated. Zenith angle = 30°.

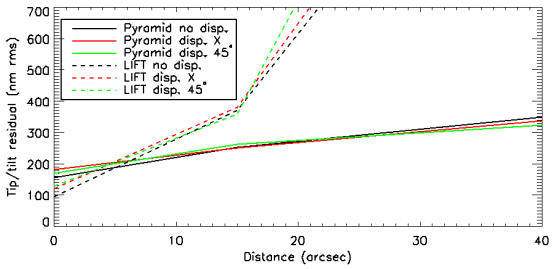

(a) Only tip/tilt estimated

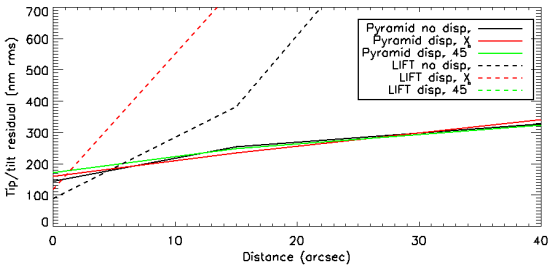

(b) Tip/tilt/focus estimated, tip/tilt res.

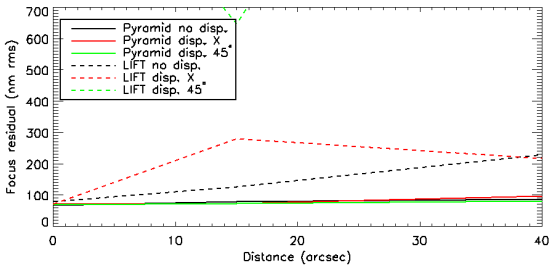

(c) Tip/tilt/focus estimated, focus res.

Figure 2. Comparison of the LO residuals obtained with LIFT or the pyramid as a function of the NGS distance for different dispersion conditions: no dispersion, dispersion along X or dispersion at 45°. Top left: Only tip/tilt estimated. Top right and bottom: tip/tilt and focus residuals when the 3 modes are estimated. Zenith angle = 60°.

As expected from the NGS mode results, the pyramid is insensitive to the chromatic dispersion. LIFT's performance is not significantly impacted either at a zenith angle of 30°, or at 60° when estimating only tip/tilt. There is a strong impact of the dispersion when estimating focus (at z = 60°), as LIFT uses the elongation of the spot due to astigmatism to compute the focus amplitude. An elongation due to other factors, such as the chromatic dispersion, can thus introduce a significant bias. The effect is mostly visible when the dispersion is at 45°, which is the direction of the spot elongation due to astigmatism. In Fig. 2, the residuals due to this dispersion are off the graph and greater than 1000 nm. This result might be improved by implementing the dispersion effects in the PSF model used in LIFT.

At z = 30°, we retrieve the results from previous works:[5] LIFT provides a significant gain over the pyramid for tip/tilt estimation on a NGS up to 15" off-axis (factor 1.5-2 in RMS), and a similar performance for focus. Going further off-axis reduces the performance due to the poor correction of the NGS by the AO system, invalidating the small phase approximation used in LIFT. The same happens when pointing at z = 60°, as the seeing increases. In this case, LIFT can provide an improvement only for tip/tilt, in good dispersion conditions and/or without estimating focus, with a NGS close to the axis.

The divergence of LIFT's tip/tilt estimation at low SRs, when only tip/tilt is estimated, is unexpected. In these conditions, LIFT is similar to a Weighted Center of Gravity (WCoG), with a Full Width at Half Maximum (FWHM) equal to the diffraction-limited spot's FWHM.[7,8] What we see here might just be an effect of the non-linearity of the WCoG, since there is no strategy to roughly recenter the weighting map on the spot in these simulations (LIFT's weighting is kept at the center of the subaperture). This also affects the case where focus is estimated, as a wrong centering of the weighting map biases the focus estimation as well. There is thus room for improvement.

The expected performance on low orders is summarized in Table 7.

Table 7. Tip/tilt and focus residuals in the best and worse cases.

		Sensor	Tip/tilt residual (nm rms)	Tip/tilt residual (mas)	Focus residual (nm rms)
z = 30°	NGS on axis (best)	LIFT	39	3.3	43
	NGS at 40" (worse)	pyramid	190	15.8	80
z = 60°	NGS on axis (best, good disp.)	LIFT	118	9.8	70
	NGS on axis (best, bad disp.)	pyramid	171	14.3	70
	NGS at 40" (worse)	pyramid	342	28.5	96

2.4 Summary

We find that the pyramid in NGS mode provides SRs in K band between 30% to 85% at z = 30°, which is consistent with our previous studies. At z = 60°, the SR ranges from 22% to 79%. We have demonstrated that the pyramid's performance would not depend on the chromatic dispersion, hence there is no need for an ADC in the design.

In LGS mode, we may want to swap the pyramid with LIFT in cases that are not too far from median conditions, with a NGS up to 15" off-axis. In other cases, the pyramid is much more stable. The residuals to expect would be from 3.3 mas (z = 30°, NGS at 0") to 28.5 mas (z = 60°, NGS at 40") on tip/tilt, and from 43 nm to 96 nm on focus (same conditions).

3. DESIGN CONSIDERATIONS

In order to aid in the design of the WFS specific simulations are carried out to assess different design choices. Here we highlight a couple of examples.

3.1 Wavefront sampling

A key choice in the WFS design is the sampling of the wavefront: the number of pixels across one of the pupil images. This will have implications for the optical design as well as the maximum frame rate of the detector (determined by the size of the SAPHIRA sub-array). The minimum sampling is set by the number of DM actuators across the pupil. Initially, for the Keck pyramid, this will be 20. However, in the second phase of KPIC[9] a high order deformable mirror will be included with 32 actuators across the pupil, requiring a sampling of at least 32 pixels.

For pyramid wavefront sensing it is often advantageous to over-sample the pupil on the detector with respect to the DM actuators. This is due to the placement of the four pupils on the detector. If the pupils are not separated by an integer number of pixels then the sampling locations for each pupil are slightly different: the pupils are shifted with respect to their equivalent pixels. This can result in a loss in sensitivity to high spatial frequency wavefronts. However, achieving an integer separation requires very tight tolerances on the angles of the pyramid faces. Another way to mitigate this effect is to oversample the wavefront, shifting the loss in sensitivity to frequencies outside the correction band.

The impact of non-integer pupil separation for different wavefront samplings is illustrated in figure 3, where the results of a simulation of the Keck pyramid are shown. The performance (K-band Strehl ratio) is simulated for deviations (shifts) from an integer pupil separation, both for a sampling matching the number of DM actuators (32 pixels) and for an over-sampled WFS (40 pixels). With small shifts the smaller sampling delivers a slightly better performance, due to lower overall noise. As the shift is increased the performance begins to degrade, with the oversampled case demonstrating greater resilience to this effect. Consequently a sampling of 40 pixels was chosen for the Keck pyramid.

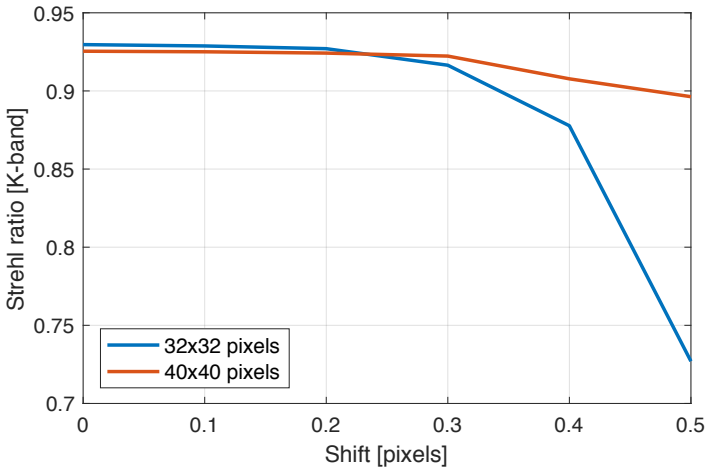

Figure 3. The simulated performance (Strehl ratio in K-band) of the Keck pyramid WFS vs. a shift in the pupil separation from an integer number of pixels. The results are shown for a sampling of 32 pixels, matching the number of DM actuators, and an oversampled case of 40 pixels.

3.2 Impact of non-common path aberrations

Another consideration during the design phase is the impact of NCPA. In most AO systems these are mitigated by applying reference signals to the WFS and closing the loop on a non-flat wavefront to optimize the image on the science instrument. For the pyramid WFS such compensation can significantly impact the behavior of the sensor, as the range is small compared with the commonly used Shack-Hartmann WFS and deviations from a diffraction-limited PSF on the tip of the prism can quickly reduce the sensitivity.

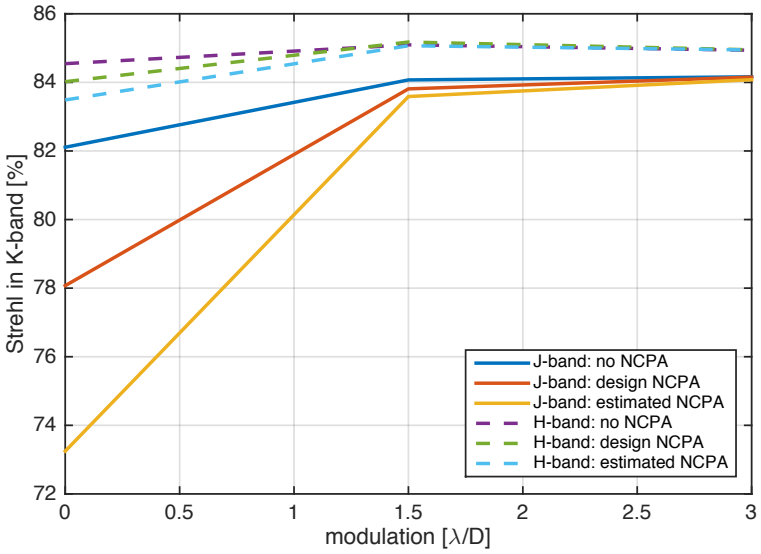

Figure 4. Simulations of the impact of NCPA on the performance (K-band Strehl ratio) of the Keck pyramid at different modulation amplitudes.

For the Keck pyramid WFS we expect some NCPA between the Pyramid WFS and NIRC2 due to a dichroic in the beam. Figure 4 shows the results of simulations of the Keck pyramid WFS with different levels of NCPA:

- No NCPA.
- Design NCPA. Includes the astigmatism induced from the dichroic, with other parameters at their nominal design values (position, curvature etc.).
- Estimated NCPA. The expected NCPA, including dichroic astigmatism and errors corresponding to design tolerances.

The system is modeled at the two potential sensing bands (J and H) and for different levels of modulation. The performance is assessed in terms of Strehl ratio in K-band.

In all cases the presence of NCPA causes a drop in performance. However, the effect is less pronounced for longer wavelengths (H-band) and with modulation. Both of these increase the range of the sensor, with a smaller effect of the presence of NCPA on the sensitivity of the WFS. This highlights advantages of doing the sensing at longer wavelengths: a slight improvement in performance and ability to use the sensor without modulation.

4. CALIBRATION

Once the Keck pyramid WFS is installed the next steps will be to close the loop on the calibration source and on-sky. The experience of other AO systems utilizing pyramid WFSs (the Larger Binocular Telescope and Subaru's extreme AO system SCExAO) have suggested that on-sky calibration of the system is crucial to realize the full potential of the Pyramid. This is due to a reduction in performance between the diffraction-limited case, such as that recorded using a calibration source, and on sky where the PSF is an AO-corrected PSF.

The Keck pyramid will operate at longer wavelengths, and so these effects are expected to be reduced as the PSF is closer to the diffraction limit. Nevertheless, the long term aim will be to implement such calibration strategies. However, initial calibration will aim to use response matrices measured using the calibration source for the first closed loop results. Here we explore the expected results of such calibration.

The pupil of the internal calibration source of Keck II is defined by the circular DM aperture. This covers a larger area than the true Keck pupil, a hexagonal pupil including the central obstruction and spiders. The overlap

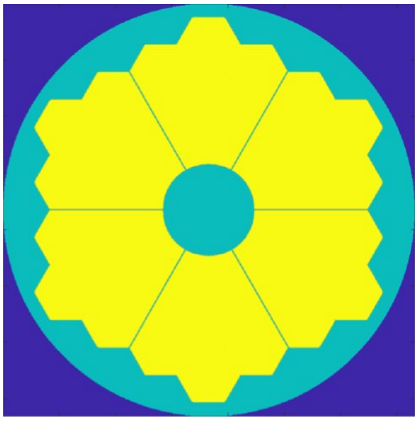

Figure 5. Overlap between the true Keck pupil and Keck DM pupil. The overlap is shown in yellow.

of the two pupils is shown in figure 5. A response matrix taken with the calibration source will over-illuminate the DM compared to the on-sky pupil. Therefore, in order to use a control matrix computed from calibration source measurements, the WFS pixels illuminated by only the calibration source (not the Keck pupil) must be removed from the response matrix.

Such a case was simulated to assess the impact of this calibration on the performance in closed loop. The initial results are shown in figure 6. The *baseline* residual phase shown here corresponds to the performance if a response matrix was measured using the true Keck pupil. This is compared with the *Keck pupil* residual phase, using the calibration source response matrix. The loop is successfully closed using this method, with a similar performance to the baseline. There are some deviations in performance, mostly coming from phase errors at the edges of the pupil. In addition, the simulation demonstrates that there is little impact on performance due to the presence of the spiders, as they are small compared to the WFS pixel size.

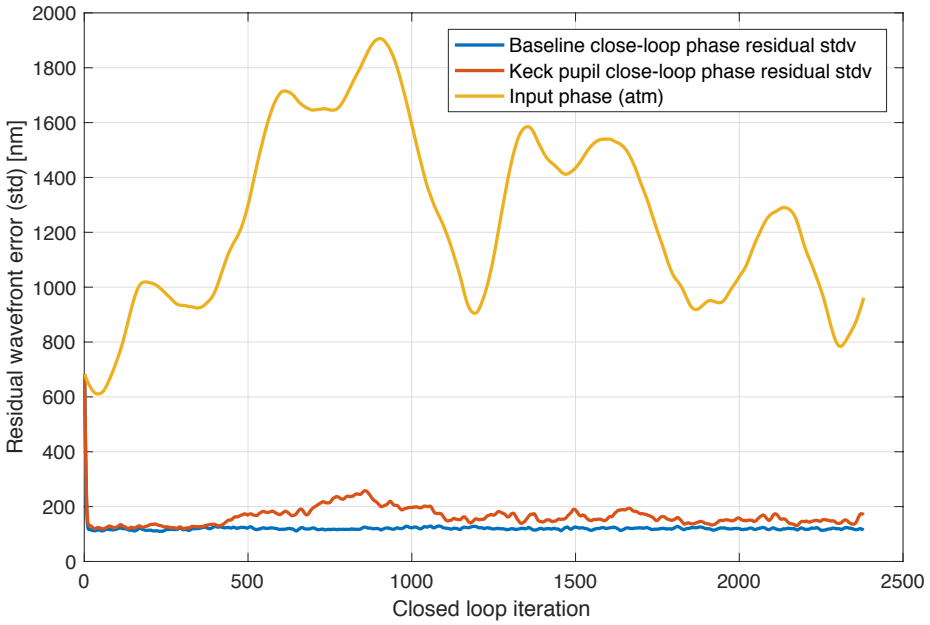

Figure 6. Simulation of the expected Keck pyramid WFS performance when the loop is closed on-sky. Different methods of calibration are compared. The *baseline* uses calibration measurements taken with the true Keck pupil. The *Keck pupil* results use calibration measurements from a simulated calibration source (with an over-sized circular pupil).

5. CONCLUSION

In median conditions (median seeing, a zenith angle of 30°), the pyramid WFS that will be implemented in Keck II should provide a Strehl ratio in K band of up to 85% at the bright end and 30% at the faint end (an H-band magnitude of 14) in NGS mode. These results are consistent with previous studies. At lower elevation (a zenith angle of 60°) these Strehl ratios become 80% and 22%. We have demonstrated that the performance of the pyramid does not depend on the atmospheric chromatic dispersion nor the dispersion from the pyramid itself. Therefore an ADC is not required.

In LGS mode, the focal-plane WFS LIFT would provide a significant improvement over the pyramid (a factor 1.5-2 in RMS) for the estimation of tip/tilt in median conditions, with a NGS up to 15" off-axis. In the same conditions the estimation of focus is similar for both sensors. At a zenith angle of 30° LIFT has some slight sensitivity to chromatic dispersion and at 60° the elongation of the spot due to dispersion can prevent the estimation of focus. In general, at low Strehl ratios (far off-axis and/or at z = 60°), LIFT's performance is significantly impacted while the pyramid is much more stable. The performance of the whole system could thus be optimized by swapping between the pyramid and LIFT according to the conditions.

In addition to this performance assessment, we have studied the parameters that affect the design and implementation of the pyramid WFS. We have shown that we can compensate the impact of mis-registrations/pupil shifts by oversampling the pupil. The sensitivity to NCPA is significantly reduced by sensing at longer wavelengths (H band) and can be further compensated by a small modulation. Finally, we have demonstrated our capability to correctly calibrate the interaction matrix of the pyramid, taking into account differences in the pupil shape between the true Keck pupil and the calibration source.

ACKNOWLEDGMENTS

This work was partly funded by INAF (Research Grant DD 27). The Keck II pyramid wavefront sensor is funded by the National Science Foundation under Grant No. AST-1611623. The W. M. Keck Observatory is operated as a scientific partnership among the California Institute of Technology, the University of California, and the National Aeronautics and Space Administration. The Observatory was made possible by the generous financial support of the W. M. Keck Foundation.

REFERENCES

[1] Wizinowich, P., Le Mignant, D., Bouchez, A. H., Campbell, R. D., Chin, J. C., Contos, A. R., van Dam, M. A., Hartman, S. K., Johansson, E. M., Lafon, R. E., et al., "The WM Keck Observatory laser guide star adaptive optics system: overview," *Publications of the Astronomical Society of the Pacific* **118**(840), 297 (2006).

[2] Ragazzoni, R., "Pupil plane wavefront sensing with an oscillating prism," *Journal of modern optics* **43**(2), 289–293 (1996).

[3] Wizinowich, P., Chun, M., Mawet, D., Agapito, G., Dekany, R., Esposito, S., Fusco, T., Guyon, O., Hall, D., Plantet, C., and Rigaut, F., "Near-infrared wavefront sensing," *Proc.SPIE* **9909**, 9909 – 9909 – 13 (2016).

[4] Feautrier, P., Gach, J.-L., and Wizinowich, P., "State of the art IR cameras for wavefront sensing using e-APD MCT arrays," in [*AO4ELT4 Proceedings*], (2015).

[5] Plantet, C., Agapito, G., Giordano, C., Esposito, S., Wizinowich, P., and Bond, C., "End-to-end simulations of a near-infrared pyramid sensor on Keck II," (01 2017).

[6] G. Agapito, A. Puglisi, S. E., "Passata: object oriented numerical simulation software for adaptive optics," *Proc.SPIE* **9909**, 9909 – 9909 – 9 (2016).

[7] Meimon, S., Fusco, T., and Mugnier, L. M., "LIFT: a focal-plane wavefront sensor for real-time low-order sensing on faint sources," *Optics letters* **35**(18), 3036–3038 (2010).

[8] Plantet, C., Meimon, S., Conan, J.-M., and Fusco, T., "Experimental validation of LIFT for estimation of low-order modes in low-flux wavefront sensing," *Optics Express* **21**, 16337–16352 (July 2013).

[9] Mawet, D., Wizinowich, P., Dekany, R., Chun, M., Hall, D., Cetre, S., Guyon, O., Wallace, J. K., Bowler, B., Liu, M., Ruane, G., Serabyn, E., Bartos, R., Wang, J., Vasisht, G., Fitzgerald, M., Skemer, A., Ireland, M., Fucik, J., Fortney, J., Crossfield, I., Hu, R., and Benneke, B., "Keck planet imager and characterizer: concept and phased implementation," in [*Proceedings of the SPIE*], **9909** (2016).